

Electron Waiting Times of a Cooper Pair Splitter

Nicklas Walldorf,¹ Ciprian Padurariu,² Antti-Pekka Jauho,¹ and Christian Flindt²

¹Center for Nanostructured Graphene (CNG), Department of Micro- and Nanotechnology, Technical University of Denmark, DK-2800 Kongens Lyngby, Denmark

²Department of Applied Physics, Aalto University, 00076 Aalto, Finland
(Dated: July 21, 2022)

Electron waiting times are an important concept in the analysis of quantum transport in nano-scale conductors. Here we show that the statistics of electron waiting times can be used to characterize Cooper pair splitters that create spatially separated spin-entangled electrons. A short waiting time between electrons tunneling into different leads is associated with the fast emission of a split Cooper pair, while long waiting times are governed by the slow injection of Cooper pairs from a superconductor. Experimentally, the waiting time distributions can be measured using real-time single-electron detectors in the regime of slow tunneling, where conventional current measurements are demanding. Our work is important for understanding the fundamental transport processes in Cooper pair splitters and the predictions may be verified using current technology.

Introduction.— Quantum technologies that exploit non-classical phenomena such as discreteness, coherence, and entanglement promise solutions to current challenges in computation, sensing, and metrology [1]. For solid-state quantum computers, an important building block is a device that can generate pairs of entangled electrons [2]. In one prominent approach, Cooper pairs in a superconductor are converted into spatially separated electrons that preserve the entanglement of their spins [3, 4]. Cooper pair splitters have been realized in experimental architectures based on superconductor–normal-state hybrid systems [5–7], InAs nanowires [8–11], carbon nanotubes [12–16], and recently graphene structures [17, 18].

The efficiency of Cooper pair splitters can be determined using conductance measurements [8–17]. For some setups, the efficiency is approaching unity [10, 14], indicating that Cooper pair splitters may be suited for electronics-based quantum technologies. One may now hope to detect the entanglement of the outgoing electrons by measuring the cross-correlations of the currents in the output channels [10, 19–21]. However, while these approaches are based on conventional current measurements, recent progress in the real-time detection of single electrons is opening another promising avenue for understanding quantum transport in nano-scale devices [22].

In this Letter we propose to characterize Cooper pair splitters using the distribution of electron waiting times. The electron waiting time is the time that passes between subsequent tunneling events. Waiting time distributions (WTDs) have in recent years been investigated for quantum transport in quantum dots [23–37], mesoscopic conductors [38–45], and superconducting devices [46–50]. Here, we show that the WTD is a sensitive tool to understand the working principle of the Cooper pair splitter in Fig. 1(a). As we discuss below, WTDs such as those in Fig. 1(b) and (c) provide clear signatures of the Cooper pair splitting. Specifically, the splitting of Cooper pairs is associated with a large peak at short times in the WTD for tunneling into different

drains, Fig. 1(c). With the ability to detect electrons participating in Andreev tunneling across normal-state–superconductor interfaces [51, 52], a measurement of the electron waiting times in a Cooper pair splitter appears feasible with current technology.

Cooper pair splitter.— The Cooper pair splitter consists of two quantum dots (QDs) coupled to a superconductor and two normal leads [4]. The grounded superconductor acts as a source of Cooper pairs. The negatively biased leads serve as drains for electrons in the QDs. Coulomb interactions are so strong that each QD

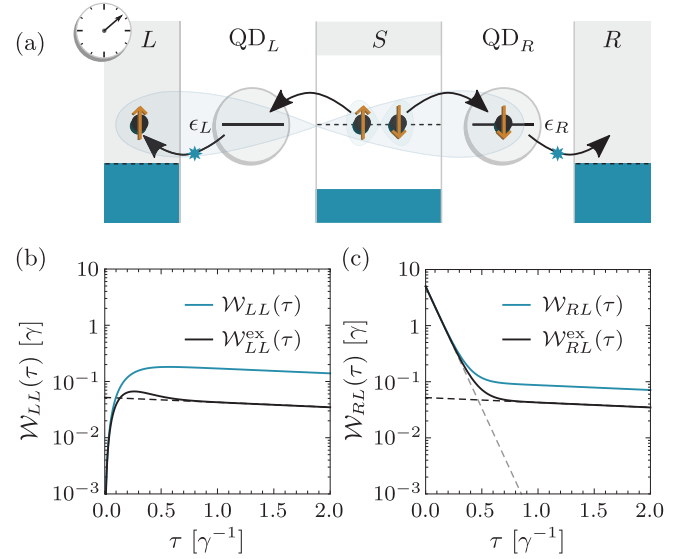


Figure 1. Electron waiting times of a Cooper pair splitter. (a) Two QDs are coupled to a superconducting source of Cooper pairs and two normal-metal leads. The detection of a tunneling event (star) starts the clock. A subsequent tunneling event stops it. WTDs for tunneling into the same/different leads are shown in panels (b) and (c). The WTDs $\mathcal{W}_{ji}(\tau)$ are evaluated using Eq. (4), and the exclusive WTDs $\mathcal{W}_{ji}^{\text{ex}}(\tau)$ are defined in Eq. (6). Parameters are $\xi := \gamma_L = \gamma_R = 10\gamma$, $\gamma_{\text{CPS}} = \gamma_{\text{EC}} = \gamma$, and $\epsilon_L = \epsilon_R = 0$. Dashed lines are exponentials with decay rates ξ (grey) and $2\gamma_{\text{CPS}}^2/\xi$ (black).

cannot be occupied by more than one electron at a time. With a large superconducting gap, we may focus on the subgap transport (the working regime is specified below). The superconductor can then be included in an effective Hamiltonian of the QDs reading [53–57]

$$\hat{H}_{\text{QDs}} = \sum_{\ell\sigma} \epsilon_{\ell} \hat{d}_{\ell\sigma}^{\dagger} \hat{d}_{\ell\sigma} - \gamma_{\text{EC}} \sum_{\sigma} \left(\hat{d}_{L\sigma}^{\dagger} \hat{d}_{R\sigma} + \text{h.c.} \right) - \frac{\gamma_{\text{CPS}}}{\sqrt{2}} \left(\hat{d}_{L\downarrow}^{\dagger} \hat{d}_{R\uparrow}^{\dagger} - \hat{d}_{L\uparrow}^{\dagger} \hat{d}_{R\downarrow}^{\dagger} + \text{h.c.} \right), \quad (1)$$

Here, the operator $\hat{d}_{\ell\sigma}^{\dagger}$ ($\hat{d}_{\ell\sigma}$) creates (annihilates) an electron in QD $_{\ell}$, $\ell \in \{L, R\}$ with spin $\sigma \in \{\uparrow, \downarrow\}$ and energy ϵ_{ℓ} relative to the chemical potential of the superconductor, $\mu_S = 0$. The amplitudes γ_{CPS} and γ_{EC} correspond to Cooper pair splitting (CPS) and elastic cotunneling (EC) processes, respectively. In the CPS processes, a Cooper pair in the superconductor is converted into two spin-entangled electrons in a singlet state with one electron in each QD, or vice versa. Such processes are favored when the empty state of the QDs is energetically degenerate with the doubly occupied state, $\epsilon_L + \epsilon_R = 0$ [58–61]. In the spin-preserving EC processes, an electron in one of the QDs is transferred via the superconductor to the other QD. These processes are on resonance when the QD levels are energetically aligned, $\epsilon_L = \epsilon_R$.

Transport through each QD is described by resonant tunneling and must be treated to all orders in the coupling to the leads. When the resonant level is deep inside the transport energy window, the transport can be described by a Markovian quantum master equation for the reduced density matrix $\hat{\rho}$ of the QDs (with $\hbar = 1$) [53, 62]

$$\frac{d}{dt} \hat{\rho} = \mathcal{L} \hat{\rho} = -i[\hat{H}_{\text{QDs}}, \hat{\rho}] + \mathcal{D} \hat{\rho}. \quad (2)$$

Here, the Liouvillian \mathcal{L} describes both coherent processes governed by \hat{H}_{QDs} , and incoherent single-electron jumps to the normal metals captured by the Lindblad dissipator

$$\mathcal{D} \hat{\rho} = \sum_{\ell\sigma} \gamma_{\ell} \left[\hat{d}_{\ell\sigma} \hat{\rho} \hat{d}_{\ell\sigma}^{\dagger} - \frac{1}{2} \{ \hat{\rho}, \hat{d}_{\ell\sigma}^{\dagger} \hat{d}_{\ell\sigma} \} \right]. \quad (3)$$

We take the rate γ_{ℓ} at which electrons leave via lead ℓ to be independent of the spin. To summarize, we work in the regime $U, \Delta \gg |V| \gg \epsilon_{\ell}, \gamma_{\ell}, \gamma_{\text{CPS}}, \gamma_{\text{EC}}$, where U is the Coulomb interaction energy, Δ is the superconducting gap, and V is the negative voltage bias. Due to the large negative bias, the electron transport from the QDs to the drain electrodes is unidirectional and the thermal smearing in the leads becomes unimportant.

Electron waiting times.— We characterize the Cooper pair splitter by considering the distribution of electron waiting times. Given that an electron with spin σ has just tunneled into lead ℓ , the electron waiting time τ is the time that passes until another electron with spin σ' tunnels into lead ℓ' . Due to the stochastic nature of

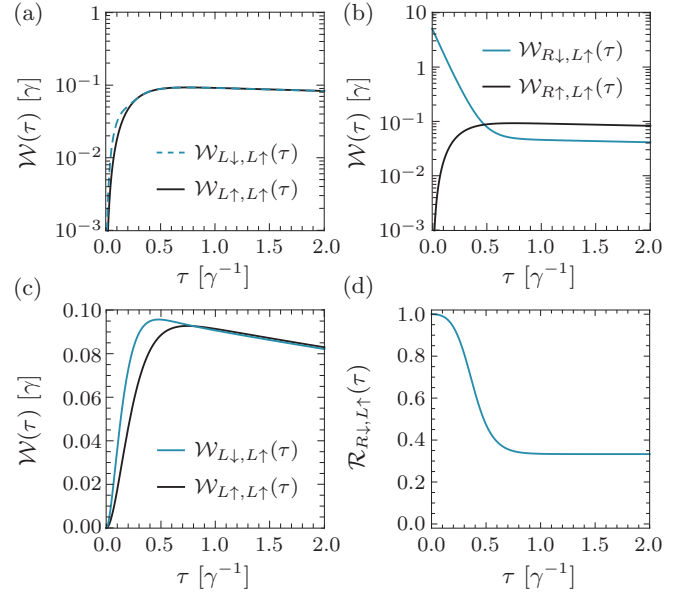


Figure 2. Spin-resolved WTDs. (a) Spin-resolved WTDs for tunneling into the same lead. (b) Spin-resolved WTDs for tunneling into different leads. In (a) and (b), the parameters are $\gamma_L = \gamma_R \equiv 10\gamma$, $\gamma_{\text{CPS}} = \gamma_{\text{EC}} = \gamma$, and $\epsilon_L = -\epsilon_R = 10\gamma$. (c) Spin-resolved WTDs for tunneling into the same lead with same parameters except that $\epsilon_L = \epsilon_R = 0$. (d) The branching ratio in Eq. (5) corresponding to the WTDs in panel (b).

the charge transport, the electron waiting time is a fluctuating quantity that must be characterized by a probability distribution. The terms in Eq. (3) of the form $\mathcal{J}_{\ell\sigma} \hat{\rho} \equiv \gamma_{\ell} \hat{d}_{\ell\sigma} \hat{\rho} \hat{d}_{\ell\sigma}^{\dagger}$ describe incoherent tunneling processes in which an electron with spin σ in QD $_{\ell}$ tunnels into lead ℓ . The distribution of waiting times between transitions of type $i = \ell\sigma$ and $j = \ell'\sigma'$ can then be expressed as [23, 43, 63]

$$\mathcal{W}_{ji}(\tau) = \frac{\text{Tr}[\mathcal{J}_j e^{(\mathcal{L} - \mathcal{J}_j)\tau} \mathcal{J}_i \hat{\rho}_S]}{\text{Tr}[\mathcal{J}_i \hat{\rho}_S]}, \quad (4)$$

where $\hat{\rho}_S$ is the stationary density matrix given as the normalized solution to the equation $\mathcal{L} \hat{\rho}_S = 0$. The expression above for the WTD can be understood as follows: after a transition of type i has occurred, the system is evolved until the next transition of type j happens. The denominator ensures that the WTD is normalized to unity when integrated over all possible waiting times. In our calculations, we express the elements of the reduced density matrix as a column vector and calculate the matrix elements of the Liouville operator from Eq. (2).

Figures 1(b) and 1(c) show WTDs for transitions into the same lead and different leads, respectively. We first disregard the spin degree of freedom. Experimentally, transitions between different charge states can be monitored using charge detectors that measure the occupation of each QD [22, 51, 52]. In Fig. 1(b), we consider the waiting time between transitions into the left lead. Here, the coupling to the drain electrodes is much larger than

the coupling to the superconductor, $\gamma_L, \gamma_R \gg \gamma_{\text{CPS}}, \gamma_{\text{EC}}$. As the QDs cannot be doubly-occupied, the WTD is strongly suppressed at short times, $\tau \ll \gamma_{\text{CPS}}^{-1}$, and vanishes completely at $\tau = 0$, since simultaneous transitions into the same lead are not possible. At long times, the WTD is governed by the slow refilling of the left QD and the subsequent tunneling of an electron into the left lead. This WTD resembles what one would expect for single-electron tunneling through a single QD without any Cooper pair splitting [23].

A very different picture emerges from the waiting time between transitions into different leads. In Fig. 1(c), the splitting of a Cooper pair is signaled by a large peak in the WTD at short times, $\tau \ll \gamma_{\text{CPS}}^{-1}$. In this case, the tunneling of an electron into the left lead is quickly followed by a transition into the right lead on a time-scale given by the coupling to the right lead, γ_R^{-1} . The slow decay of the WTD describes the waiting time between the last electron originating from one Cooper pair and the first electron originating from the next Cooper pair. This WTD clearly reflects the non-local nature of the CPS processes and it carries information about the *short* waiting times between electrons from the *same* Cooper pair and the *long* waiting times between electrons originating from *different* Cooper pairs. Experimentally, a measurement of the WTD in Fig. 1(c) would constitute a strong evidence of efficient Cooper pair splitting.

Spin-resolved WTDs.— The splitting of Cooper pairs can be identified in the charge-resolved WTDs shown in Fig. 1(c). Still, further information can be obtained from the spin-resolved WTDs. Experimentally, one might measure spin-resolved WTDs using ferromagnetic detectors [55, 64, 65]. In Fig. 2, we show WTDs that are resolved with respect to the spin degree of freedom. In Figs. 2(a) and (b), the levels are detuned so that only CPS processes are on resonance. Again, the WTDs for transitions into the same lead show essentially no signatures of the CPS processes. By contrast, the CPS processes can be identified in the WTD in Fig. 2(b) for transitions into different leads. Here, the CPS processes show up as a large enhancement at short times in the WTD for opposite spins. Due to the splitting of a Cooper pair, the tunneling of a spin-up electron into the left lead is likely followed by the tunneling of a spin-down electron into the right lead. A similar enhancement is not found for electrons with the same spin, since they must originate from different Cooper pairs.

In Fig. 2(c), both the CPS and EC processes are tuned into resonance. The combination of these processes lead to an enhancement at intermediate times in the WTD for electrons with opposite spins tunneling into the same lead. In this case, two electrons from a Cooper pair can exit into the same drain due to a spin-preserving EC process that transfers the second electron from the right to the left QD before it exists via the left drain. This is not possible for electrons with the same spin, since

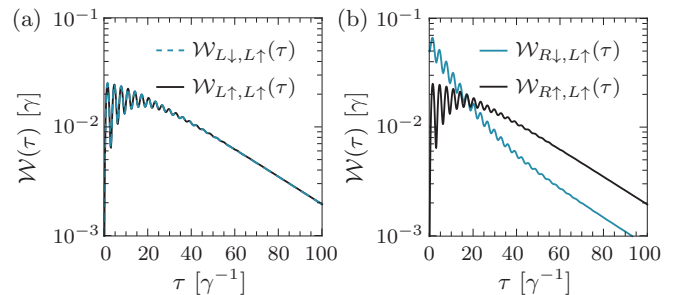


Figure 3. Coherent oscillations. (a) Spin-resolved WTDs for tunneling into the same lead. (b) Spin-resolved WTDs for tunneling into different leads. In both panels, the parameters are $\gamma_L = \gamma_R \equiv 0.1\gamma$, $\gamma_{\text{CPS}} = \gamma_{\text{EC}} = \gamma$, and $\epsilon_L = -\epsilon_R = 10\gamma$.

they cannot originate from the same Cooper pair, and the corresponding WTD is not enhanced in a similar way.

Importantly, from the spin-resolved WTDs, we can evaluate the branching ratio of the spins defined as

$$\mathcal{R}_{R\downarrow, L\uparrow}(\tau) \equiv \frac{\mathcal{W}_{R\downarrow, L\uparrow}(\tau)}{\mathcal{W}_{R\downarrow, L\uparrow}(\tau) + \mathcal{W}_{R\uparrow, L\uparrow}(\tau)}. \quad (5)$$

The branching ratio is the probability that two electrons, which tunnel into different leads separated by the waiting time τ , have opposite spins. Figure 2(d) shows that it is highly probable that electrons separated by a short waiting time have opposite spins and they likely originate from the same Cooper pair. This finding is important since it allows us to conclude that the large peak in Fig. 1(c) with near-unity probability corresponds to opposite spins originating from the same Cooper pair [66].

Until now, we have focused on the situation where the coupling to the drains is much larger than the coupling to the superconductor. This regime may be most attractive for efficient Cooper pair splitting, since the split pair of electrons is quickly transferred to the drain electrodes. However, the opposite regime, $\gamma_{\text{CPS}}, \gamma_{\text{EC}} \gg \gamma_L, \gamma_R$, is also interesting. In Fig. 3, the levels are tuned so that only the CPS processes are on resonance. In Fig. 3(a), we then see oscillations in the WTDs due to CPS processes between the superconductor and the QDs [23, 27, 46]. The same behavior can be observed in the WTD for tunneling into different leads, Fig. 3(b). However, the WTD for opposite spins is different, since in this case the two electrons could also originate from the same Cooper pair. The oscillations are superimposed on an exponential decay due to the waiting time between electrons from the same Cooper pair. The possibility of detecting coherent oscillations in WTDs is discussed in Ref. [46].

Exclusive WTDs.— To better understand the time-scales that enter the WTDs, we introduce *exclusive* WTDs. Again, we consider the waiting time that passes between transitions of types i and j . However, we now exclude cases, where any other transitions occur during

the waiting time. This WTD is then defined as [23, 46]

$$\mathcal{W}_{ji}^{\text{ex}}(\tau) = \frac{\text{Tr}[\mathcal{J}_j e^{\mathcal{L}^{\text{ex}} \tau} \mathcal{J}_i \hat{\rho}_S]}{\text{Tr}[\mathcal{J}_i \hat{\rho}_S]}, \quad (6)$$

where $\mathcal{L}^{\text{ex}} = \mathcal{L} - \sum_k \mathcal{J}_k$ removes all possible transitions from the full time evolution given by \mathcal{L} . In contrast to the WTD in Eq. (4), the exclusive WTD is only normalised upon integrating over all waiting times *and* summing over all types of final events. Due to its simpler structure, the exclusive WTD can be evaluated analytically. For example, with $\gamma_L = \gamma_R = \xi$ and $\epsilon_L = -\epsilon_R = \epsilon$, we find

$$\begin{aligned} \mathcal{W}_{\ell\sigma, \bar{\ell}\bar{\sigma}}^{\text{ex}}(\tau) &= \frac{\xi}{2} e^{-\xi\tau} + 2\mathcal{W}_{\ell\sigma, \ell\sigma}^{\text{ex}}(\tau) - \mathcal{W}_{\ell\sigma, \ell\bar{\sigma}}^{\text{ex}}(\tau), \\ \mathcal{W}_{\ell\sigma, \ell'\sigma}^{\text{ex}}(\tau) &= \frac{\xi}{2} e^{-\xi\tau} \alpha_{\text{CPS}}^2 [1 - \cos(\omega_{\text{CPS}}\tau)], \\ \mathcal{W}_{\ell\sigma, \ell\bar{\sigma}}^{\text{ex}}(\tau) &= \xi e^{-\xi\tau} \alpha_{\text{EC}}^2 [1 - \cos(\omega_{\text{EC}}\tau)] + \mathcal{W}_{\ell\sigma, \ell\sigma}^{\text{ex}}(\tau), \end{aligned} \quad (7)$$

with $\bar{L} = R$ and $\bar{\uparrow} = \downarrow$ and vice versa, and we have identified the frequencies $\omega_{\text{CPS}} = 2\sqrt{\gamma_{\text{CPS}}^2 - (\xi/2)^2}$ and $\omega_{\text{EC}} = 2\sqrt{\gamma_{\text{EC}}^2 + \epsilon^2}$ associated with the coherent CPS and EC processes and introduced the ratios $\alpha_{\text{CPS}} = \gamma_{\text{CPS}}/\omega_{\text{CPS}}$ and $\alpha_{\text{EC}} = \gamma_{\text{EC}}/\omega_{\text{EC}}$. If $\gamma_{\text{CPS}} \gg \gamma_L, \gamma_R$, the WTD exhibits oscillations with frequency $\omega_{\text{CPS}} \simeq 2\gamma_{\text{CPS}}$ as seen in Fig. 3. By contrast, for $\gamma_{\text{CPS}} \ll \gamma_L, \gamma_R$, the frequency becomes imaginary and now rather corresponds to an exponential decay as in Fig. 2. In Fig. 1, we show the exclusive WTDs $\mathcal{W}_{\ell\ell'}^{\text{ex}}(\tau) = \sum_{\sigma, \sigma'} \mathcal{W}_{\ell\sigma, \ell'\sigma'}^{\text{ex}}(\tau)/2$ and their asymptotic behaviors for short and long waiting times.

Joint WTDs.— The WTDs concern waiting times between subsequent tunneling events. However, they do not describe correlations between consecutive waiting times. Such correlations can be characterized by evaluating the joint distribution of electron waiting times [43, 48]

$$\mathcal{W}_{kji}(\tau_1, \tau_2) = \frac{\text{Tr}[\mathcal{J}_k e^{(\mathcal{L} - \mathcal{J}_k)\tau_2} \mathcal{J}_j e^{(\mathcal{L} - \mathcal{J}_j)\tau_1} \mathcal{J}_i \hat{\rho}_S]}{\text{Tr}[\mathcal{J}_i \hat{\rho}_S]}, \quad (8)$$

which generalizes Eq. (4) to subsequent waiting times between transitions of type i , j , and k . For uncorrelated waiting times, the joint distribution factorizes as $\mathcal{W}_{kj}(\tau_2)\mathcal{W}_{ji}(\tau_1)$ in terms of the individual WTDs. Correlations can be quantified by the correlation function

$$\Delta\mathcal{W}_{kji}(\tau_1, \tau_2) = \frac{\mathcal{W}_{kji}(\tau_1, \tau_2) - \mathcal{W}_{kj}(\tau_2)\mathcal{W}_{ji}(\tau_1)}{\mathcal{W}_{kj}(\tau_2)\mathcal{W}_{ji}(\tau_1)}, \quad (9)$$

which is positive (negative) for positively (negatively) correlated waiting times and zero without correlations.

Figure 4 shows joint WTDs for electrons arriving in different leads together with the corresponding correlation functions. In panels (a) and (b), the coupling to the drain electrodes is much larger than the coupling to the superconductor and electrons in the QDs quickly escape to the drains. In this case, it is likely that a short waiting time between tunneling events into different electrodes is

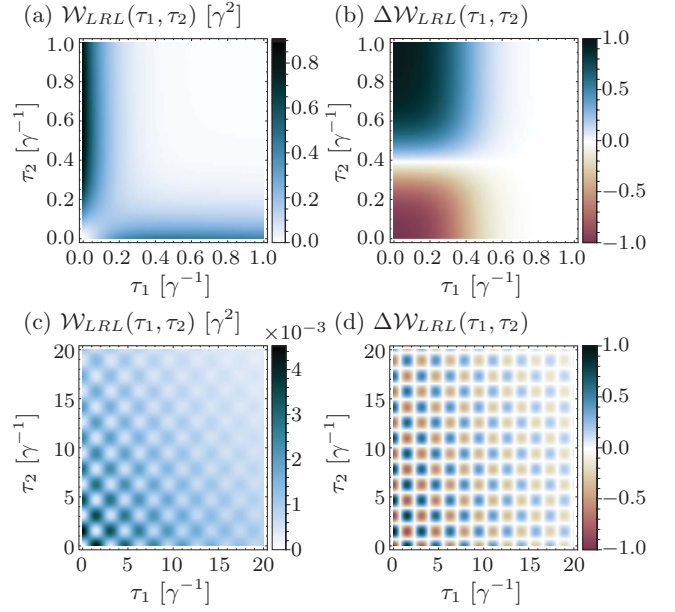


Figure 4. Joint WTDs and correlation functions. In panels (a) and (b), the parameters are $\gamma_L = \gamma_R = 10\gamma$, $\gamma_{\text{CPS}} = \gamma_{\text{EC}} \equiv \gamma$, and $\epsilon_L = \epsilon_R = 0$. In panels (c) and (d), the parameters are $\gamma_L = \gamma_R = 0.1\gamma$, $\gamma_{\text{CPS}} = \gamma_{\text{EC}} = \gamma$, and $\epsilon_L = \epsilon_R = 0$.

followed by a long waiting time until the next tunneling event occurs. The short waiting time corresponds to two electrons originating from the same Cooper pair, while the long waiting time is determined by the slow refilling of the QDs due to the next Cooper pair. It is unlikely to observe two short waiting times one after another. A similar behavior can be observed in panels (c) and (d), where the coupling to the superconductor is the largest. However, now we also see the effects of CPS and EC processes which are on resonance. In this regime, the CPS and EC processes give rise to the oscillatory pattern with frequencies governed by their coupling amplitudes.

Conclusions.— We have proposed to use waiting time distributions to characterize Cooper pair splitters. The non-local nature of the Cooper pair splitting can be clearly identified in the distribution of waiting times. Based on the recent progress in the real-time detection of Andreev tunneling, our predictions should be accessible in future experiments. Specifically, a measurement of the WTD would constitute a strong evidence of efficient Cooper pair splitting in the regime of slow tunneling, where conventional current measurements are demanding. Theoretically, it would be interesting to formulate a Bell-like inequality for the waiting time distributions to certify the entanglement of the split Cooper pairs.

We thank P. J. Hakonen, G. B. Lesovik, M. V. Moskalets, J. P. Pekola, and B. Sothmann for valuable discussions. Authors at Aalto are associated with Centre for Quantum Engineering. The Center for Nanostructured Graphene (CNG) is sponsored by the Danish Research Foundation, Project DNR103.

-
- [1] A. Zagorskin, *Quantum Engineering: Theory and Design of Quantum Coherent Structures* (Cambridge University Press, 2011).
- [2] T. D. Ladd, F. Jelezko, R. Laflamme, Y. Nakamura, C. Monroe, and J. L. O'Brien, "Review: Quantum computers," *Nature* **464**, 45 (2010).
- [3] G. B. Lesovik, T. Martin, and G. Blatter, "Electronic entanglement in the vicinity of a superconductor," *Eur. Phys. J. B* **24**, 287 (2001).
- [4] P. Recher, E. V. Sukhorukov, and D. Loss, "Andreev tunneling, Coulomb blockade, and resonant transport of nonlocal spin-entangled electrons," *Phys. Rev. B* **63**, 165314 (2001).
- [5] D. Beckmann, H. B. Weber, and H. v. Löhneysen, "Evidence for Crossed Andreev Reflection in Superconductor-Ferromagnet Hybrid Structures," *Phys. Rev. Lett.* **93**, 197003 (2004).
- [6] S. Russo, M. Kroug, T. M. Klapwijk, and A. F. Morpurgo, "Experimental Observation of Bias-Dependent Nonlocal Andreev Reflection," *Phys. Rev. Lett.* **95**, 027002 (2005).
- [7] R. S. Deacon, A. Oiwa, J. Sailer, S. Baba, Y. Kanai, K. Shibata, K. Hirakawa, and S. Tarucha, "Cooper pair splitting in parallel quantum dot Josephson junctions," *Nat. Commun.* **6**, 7446 (2015).
- [8] L. Hofstetter, S. Csonka, J. Nygård, and C. Schönenberger, "Cooper pair splitter realized in a two-quantum-dot Y-junction," *Nature* **461**, 960 (2009).
- [9] L. Hofstetter, S. Csonka, A. Baumgartner, G. Fülöp, S. d'Hollosy, J. Nygård, and C. Schönenberger, "Finite-Bias Cooper Pair Splitting," *Phys. Rev. Lett.* **107**, 136801 (2011).
- [10] A. Das, R. Ronen, M. Heiblum, D. Mahalu, A. V. Kretinin, and H. Shtrikman, "High-efficiency Cooper pair splitting demonstrated by two-particle conductance resonance and positive noise cross-correlation," *Nat. Commun.* **3**, 1165 (2012).
- [11] G. Fülöp, F. Domínguez, S. d'Hollosy, A. Baumgartner, P. Makk, M. H. Madsen, V. A. Guzenko, J. Nygård, C. Schönenberger, A. Levy Yeyati, and S. Csonka, "Magnetic Field Tuning and Quantum Interference in a Cooper Pair Splitter," *Phys. Rev. Lett.* **115**, 227003 (2015).
- [12] L. G. Herrmann, F. Portier, P. Roche, A. Levy Yeyati, T. Kontos, and C. Strunk, "Carbon Nanotubes as Cooper-Pair Beam Splitters," *Phys. Rev. Lett.* **104**, 026801 (2010).
- [13] L. G. Herrmann, P. Buset, W. J. Herrera, F. Portier, P. Roche, C. Strunk, A. Levy Yeyati, and T. Kontos, "Spectroscopy of non-local superconducting correlations in a double quantum dot," (2012), [arXiv:1205.1972](https://arxiv.org/abs/1205.1972).
- [14] J. Schindele, A. Baumgartner, and C. Schönenberger, "Near-Unity Cooper Pair Splitting Efficiency," *Phys. Rev. Lett.* **109**, 157002 (2012).
- [15] G. Fülöp, S. d'Hollosy, A. Baumgartner, P. Makk, V. A. Guzenko, M. H. Madsen, J. Nygård, C. Schönenberger, and S. Csonka, "Local electrical tuning of the nonlocal signals in a Cooper pair splitter," *Phys. Rev. B* **90**, 235412 (2014).
- [16] J. Schindele, A. Baumgartner, R. Maurand, M. Weiss, and C. Schönenberger, "Nonlocal spectroscopy of Andreev bound states," *Phys. Rev. B* **89**, 045422 (2014).
- [17] Z. B. Tan, D. Cox, T. Nieminen, P. Lähteenmäki, D. Golubev, G. B. Lesovik, and P. J. Hakonen, "Cooper Pair Splitting by Means of Graphene Quantum Dots," *Phys. Rev. Lett.* **114**, 096602 (2015).
- [18] I. V. Borzenets, Y. Shimazaki, G. F. Jones, M. F. Craciun, S. Russo, M. Yamamoto, and S. Tarucha, "High Efficiency CVD Graphene-lead (Pb) Cooper Pair Splitter," *Sci. Rep.* **6**, 23051 (2016).
- [19] S. Kawabata, "Test of Bell's Inequality using the Spin Filter Effect in Ferromagnetic Semiconductor Microstructures," *J. Phys. Soc. Japan* **70**, 1210 (2001).
- [20] N. M. Chtchelkatchev, G. Blatter, G. B. Lesovik, and T. Martin, "Bell inequalities and entanglement in solid-state devices," *Phys. Rev. B* **66**, 161320 (2002).
- [21] O. Sauret, T. Martin, and D. Feinberg, "Spin-current noise and Bell inequalities in a realistic superconductor-quantum dot entangler," *Phys. Rev. B* **72**, 024544 (2005).
- [22] S. Gustavsson, R. Leturcq, M. Studer, I. Shorubalko, T. Ihn, K. Ensslin, D. C. Driscoll, and A. C. Gossard, "Electron counting in quantum dots," *Surf. Sci. Rep.* **64**, 191 (2009).
- [23] T. Brandes, "Waiting times and noise in single particle transport," *Ann. Phys.* **17**, 477 (2008).
- [24] S. Welack, M. Esposito, U. Harbola, and S. Mukamel, "Interference effects in the counting statistics of electron transfers through a double quantum dot," *Phys. Rev. B* **77**, 195315 (2008).
- [25] S. Welack, S. Mukamel, and Y. J. Yan, "Waiting time distributions of electron transfers through quantum dot Aharonov-Bohm interferometers," *Europhys. Lett.* **85**, 57008 (2009).
- [26] M. Albert, C. Flindt, and M. Büttiker, "Distributions of Waiting Times of Dynamic Single-Electron Emitters," *Phys. Rev. Lett.* **107**, 086805 (2011).
- [27] K. H. Thomas and C. Flindt, "Electron waiting times in non-Markovian quantum transport," *Phys. Rev. B* **87**, 121405 (2013).
- [28] G.-M. Tang, F. Xu, and J. Wang, "Waiting time distribution of quantum electronic transport in the transient regime," *Phys. Rev. B* **89**, 205310 (2014).
- [29] G.-M. Tang and J. Wang, "Full-counting statistics of charge and spin transport in the transient regime: A nonequilibrium Green's function approach," *Phys. Rev. B* **90**, 195422 (2014).
- [30] B. Sothmann, "Electronic waiting-time distribution of a quantum-dot spin valve," *Phys. Rev. B* **90**, 155315 (2014).
- [31] R. Seoane Souto, R. Avriller, R. C. Monreal, A. Martín-Rodero, and A. Levy Yeyati, "Transient dynamics and waiting time distribution of molecular junctions in the polaronic regime," *Phys. Rev. B* **92**, 125435 (2015).
- [32] V. Talbo, J. Mateos, S. Retailleau, P. Dollfus, and T. González, "Time-dependent shot noise in multi-level quantum dot-based single-electron devices," *Semicond. Sci. Technol.* **30**, 055002 (2015).
- [33] S. L. Rudge and D. S. Kosov, "Distribution of residence times as a marker to distinguish different pathways for quantum transport," *Phys. Rev. E* **94**, 042134 (2016).
- [34] S. L. Rudge and D. S. Kosov, "Distribution of tunnelling times for quantum electron transport," *J. Chem. Phys.* **144**, 124105 (2016).
- [35] K. Ptaszyński, "Nonrenewal statistics in transport through quantum dots," *Phys. Rev. B* **95**, 045306 (2017).
- [36] E. Potanina and C. Flindt, "Electron waiting times of a

- periodically driven single-electron turnstile,” *Phys. Rev. B* **96**, 045420 (2017).
- [37] D. S. Kosov, “Non-renewal statistics for electron transport in a molecular junction with electron-vibration interaction,” *arXiv:1706.07295* (2017).
- [38] M. Albert, G. Haack, C. Flindt, and M. Büttiker, “Electron Waiting Times in Mesoscopic Conductors,” *Phys. Rev. Lett.* **108**, 186806 (2012).
- [39] G. Haack, M. Albert, and C. Flindt, “Distributions of electron waiting times in quantum-coherent conductors,” *Phys. Rev. B* **90**, 205429 (2014).
- [40] K. H. Thomas and C. Flindt, “Waiting time distributions of noninteracting fermions on a tight-binding chain,” *Phys. Rev. B* **89**, 245420 (2014).
- [41] D. Dasenbrook, C. Flindt, and M. Büttiker, “Floquet Theory of Electron Waiting Times in Quantum-Coherent Conductors,” *Phys. Rev. Lett.* **112**, 146801 (2014).
- [42] M. Albert and P. Devillard, “Waiting time distribution for trains of quantized electron pulses,” *Phys. Rev. B* **90**, 035431 (2014).
- [43] D. Dasenbrook, P. P. Hofer, and C. Flindt, “Electron waiting times in coherent conductors are correlated,” *Phys. Rev. B* **91**, 195420 (2015).
- [44] D. Dasenbrook and C. Flindt, “Quantum theory of an electron waiting time clock,” *Phys. Rev. B* **93**, 245409 (2016).
- [45] P. P. Hofer, D. Dasenbrook, and C. Flindt, “Electron waiting times for the mesoscopic capacitor,” *Physica E* **82**, 11 (2016).
- [46] L. Rajabi, C. Pörtl, and M. Governale, “Waiting Time Distributions for the Transport through a Quantum-Dot Tunnel Coupled to One Normal and One Superconducting Lead,” *Phys. Rev. Lett.* **111**, 067002 (2013).
- [47] S. Dambach, B. Kubala, V. Gramich, and J. Ankerhold, “Time-resolved statistics of nonclassical light in Josephson photonics,” *Phys. Rev. B* **92**, 054508 (2015).
- [48] S. Dambach, B. Kubala, and J. Ankerhold, “Time-resolved statistics of photon pairs in two-cavity Josephson photonics,” *Fortschr. Phys.* **65**, 1600061 (2017).
- [49] M. Albert, D. Chevallier, and P. Devillard, “Waiting times of entangled electrons in normal-superconducting junctions,” *Physica E* **76**, 215 (2016).
- [50] D. Chevallier, M. Albert, and P. Devillard, “Probing Majorana and Andreev bound states with waiting times,” *Europhys. Lett.* **116**, 27005 (2016).
- [51] V. F. Maisi, O.-P. Saira, Yu. A. Pashkin, J. S. Tsai, D. V. Averin, and J. P. Pekola, “Real-Time Observation of Discrete Andreev Tunneling Events,” *Phys. Rev. Lett.* **106**, 217003 (2011).
- [52] V. F. Maisi, D. Kambly, C. Flindt, and J. P. Pekola, “Full Counting Statistics of Andreev Tunneling,” *Phys. Rev. Lett.* **112**, 036801 (2014).
- [53] O. Sauret, D. Feinberg, and T. Martin, “Quantum master equations for the superconductor-quantum dot entangler,” *Phys. Rev. B* **70**, 245313 (2004).
- [54] J. Eldridge, M. G. Pala, M. Governale, and J. König, “Superconducting proximity effect in interacting double-dot systems,” *Phys. Rev. B* **82**, 184507 (2010).
- [55] P. Trocha and I. Weymann, “Spin-resolved Andreev transport through double-quantum-dot Cooper pair splitters,” *Phys. Rev. B* **91**, 235424 (2015).
- [56] E. Amitai, R. P. Tiwari, S. Walter, T. L. Schmidt, and S. E. Nigg, “Nonlocal quantum state engineering with the Cooper pair splitter beyond the Coulomb blockade regime,” *Phys. Rev. B* **93**, 075421 (2016).
- [57] R. Hussein, A. Braggio, and M. Governale, “Entanglement-symmetry control in a quantum-dot Cooper-pair splitter,” *Phys. Status Solidi B* **254**, 1600603 (2017).
- [58] D. Chevallier, J. Rech, T. Jonckheere, and T. Martin, “Current and noise correlations in a double-dot Cooper-pair beam splitter,” *Phys. Rev. B* **83**, 125421 (2011).
- [59] B. Hiltcher, M. Governale, J. Splettstoesser, and J. König, “Adiabatic pumping in a double-dot Cooper-pair beam splitter,” *Phys. Rev. B* **84**, 155403 (2011).
- [60] M. Flöser, D. Feinberg, and R. Mélin, “Absence of split pairs in cross correlations of a highly transparent normal metal-superconductor-normal metal electron-beam splitter,” *Phys. Rev. B* **88**, 094517 (2013).
- [61] I. A. Sadovskyy, G. B. Lesovik, and V. M. Vinokur, “Unitary limit in crossed Andreev transport,” *New J. Phys.* **17**, 103016 (2015).
- [62] Sh. Gurvitz, “Wave-function approach to Master equations for quantum transport and measurement,” *Front. Phys.* **12**, 120303 (2016).
- [63] H. J. Carmichael, S. Singh, R. Vyas, and P. R. Rice, “Photoelectron waiting times and atomic state reduction in resonance fluorescence,” *Phys. Rev. A* **39**, 1200 (1989).
- [64] O. Malkoc, C. Bergenfeldt, and P. Samuelsson, “Full counting statistics of generic spin entangler with quantum dot-ferromagnet detectors,” *Europhys. Lett.* **105**, 47013 (2014).
- [65] P. Busz, D. Tomaszewski, and J. Martinek, “Spin correlation and entanglement detection in Cooper pair splitters by current measurements using magnetic detectors,” *Phys. Rev. B* **96**, 064520 (2017).
- [66] Z. Scherübl, A. Pályi, and S. Csonka, “Probing individual split Cooper pairs using the spin qubit toolkit,” *Phys. Rev. B* **89**, 205439 (2014).